Mendeleev
Communications

Mendeleev Commun., 2025, **35**, 746–748

The role of diglyme and tetraglyme in the formation of ion transport pathways in gel electrolytes based on polyethylene glycol diacrylate

Nikita A. Slesarenko,*[a] Alexander V. Chernyak,[a,b] Vitaly I. Volkov,[a] Kyunsilu G. Khatmullina,[a,c] Alena V. Yudina,[a] Galiya Z. Tulibaeva,[a] Anna A. Slesarenko,[a] Guzaliya R. Baymuratova,[a] Alexander F. Shestakov[a,d] and Olga V. Yarmolenko*[a]

[a] *Federal Research Center of Problems of Chemical Physics and Medicinal Chemistry, Russian Academy of Sciences, 142432 Chernogolovka, Moscow Region, Russian Federation. E-mail: n.slesarenko@icp.ac.ru; oyarm@mail.ru*
[b] *Yu. A. Osipyan Institute of Solid State Physics, Russian Academy of Sciences, 142432 Chernogolovka, Moscow Region, Russian Federation*
[c] *National Research University 'Moscow Power Engineering Institute', 111250 Moscow, Russian Federation*
[d] *Department of Fundamental Physical and Chemical Engineering, M. V. Lomonosov Moscow State University, 119991 Moscow, Russian Federation*

DOI: 10.71267/mencom.7792

The methods of ^{7}Li spin relaxation and pulsed field gradient NMR were used to reveal the features of local transport of Li$^+$ cations in two polymer gel electrolytes containing an ionic liquid, the salt LiBF$_4$ and a solvent, diglyme (G2) or tetraglyme (G4). It was found that the macroscopic mass transfer of Li$^+$ cations is affected by their solvate environment from both glyme solvents and the polymer matrix. In the presence of G4, a denser three-dimensional network is formed, hindering the transport of all ions.

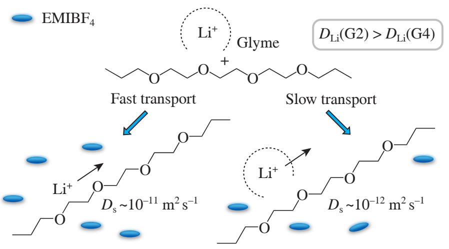

Keywords: ^{7}Li spin relaxation, PFG NMR, LiBF$_4$, diglyme, tetraglyme, electrochemical impedance, lithium anode, conductivity, diffusion coefficient.

Despite the considerable interest in polymer electrolytes, the mechanisms of ion transport in these materials are still not well understood. To elucidate this, it is essential to investigate the mobility of cations at different spatial scales. Nuclear spin relaxation and pulsed field gradient (PFG) NMR are very attractive methods for elucidating molecular and ionic mobility in a polymer electrolyte.[1–4]

This work is a continuation of a series of studies[5–7] on polymer gel electrolytes (PGEs) based on polyethylene glycol diacrylate (PEGDA) and the ionic liquid (IL) 1-ethyl-3-methylimidazolium tetrafluoroborate (EMIBF$_4$). ILs are molten salts characterized by high thermal stability, non-volatility and high ionic conductivity.[8] These features have allowed researchers to replace unsafe organic solvents in PGEs with ILs, especially for lithium batteries, where the ions providing conductivity are Li$^+$ cations.[9–11] However, the introduction of ILs also has disadvantages, such as low transport numbers for Li$^+$ cations due to competitive ion transport.[12,13] It was shown[5] that in PGEs consisting of PEGDA, EMIBF$_4$ and LiBF$_4$ with the addition of ethylene carbonate the diffusion coefficients of lithium were low. Therefore, in order to find more favorable transport pathways for Li$^+$ cations, the effect of diglyme (G2) and tetraglyme (G4) on the formation of ion transport pathways in this system was investigated. The choice of glyme solvents is due to the absence of reactive functional groups in aprotic saturated polyethers, which makes them chemically inert. Ether oxygens provide glymes with exceptional cation solvation properties,[14,15] and the polymer matrix of polyethylene glycol also serves as an analog to glymes, which will also facilitate the transport of Li$^+$ cations.

Similar to the previous work,[5] we applied radical polymerization of PEGDA in IL medium to obtain films of two PGEs: PGE1 containing 32, 4, 52 and 12 wt% PEGDA, LiBF$_4$, EMIBF$_4$ and G2 (molar ratio 1 : 1 : 6 : 2) and PGE2 containing 32, 4, 54 and 10 wt% PEGDA, LiBF$_4$, EMIBF$_4$ and G4 (molar ratio 1 : 1 : 6 : 1), respectively.

We applied spin relaxation and PFG NMR on ^{7}Li nuclei. This revealed features of cation transport in the PGE membrane at different spatial scales.† The procedure for measuring the diffusion coefficient was described previously.[16,17]

The temperature dependences of the diffusion coefficients (D_s) observed in all PGE formulations using different nuclei, such as ^{1}H of EMI$^+$ cations and solvent molecules, ^{7}Li of lithium cations and ^{19}F of BF$_4^-$ anions (Figure 1), provide information on the mobility of the corresponding ions and molecules. The diffusion attenuation obtained on ^{7}Li nuclei is not exponential and can be approximated by the sum of two exponents corresponding to the D_s values of fast and slow diffusion (Table S1),† but Figure 1(*a*) shows a weighted average D_s value.

In the temperature range from 0 to 60 °C, the diffusion coefficients measured on all nuclei for the PGE2 electrolyte with G4 are lower than those for PGE1 with G2. This phenomenon may be due to the enhanced cross-linking of the polymer matrix in the presence of G4, which is an analog of polyethylene glycol. This hypothesis is supported by the DSC data (Figure S2),† which demonstrates

---

† For details, see Online Supplementary Materials.

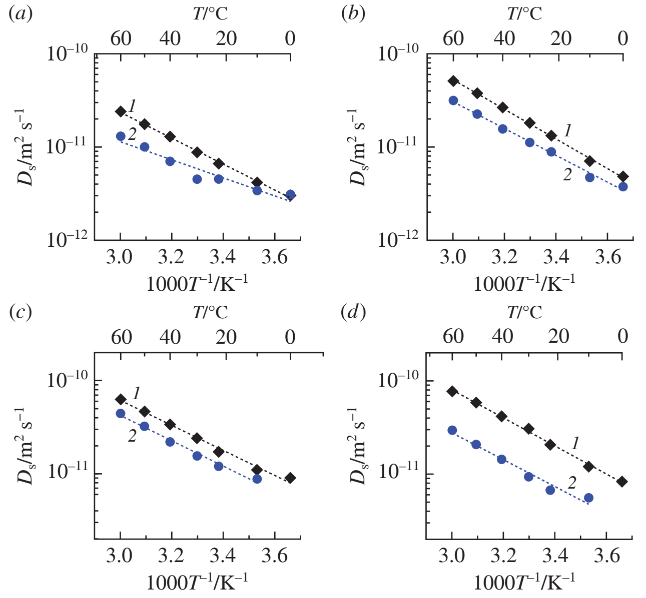

Figure 1 Temperature dependences of diffusion coefficients D_s measured using nuclei of (*a*) ^{7}Li, (*b*) ^{19}F, (*c*) ^{1}H of EMI$^+$ and (*d*) ^{1}H of solvates in the temperature range from 0 to 60 °C for (*1*) PGE1 and (*2*) PGE2.

that the glass transition temperature of PGE2 is 11 °C higher, suggesting a more ordered structure.

The temperature dependence of the conductivity of PGE [Figure 2(*a*)], measured by the electrochemical impedance spectroscopy (EIS) in cells with stainless steel (SS) blocking electrodes, has an Arrhenius shape.† As can be seen, there is a tendency for the conductivity of the PGE composition with G4 to decrease in the temperature range from 20 to 60 °C. Figure 2(*b*) demonstrates the temperature dependences of the diffusion coefficients measured using ^{7}Li nuclei for fast and slow diffusion in the temperature range from 0 to 60 °C. These plots also have an Arrhenius shape. From the data presented in Figure 2, the effective activation energies were calculated (Table 1). It appears that the activation energy of the 'fast' diffusion coefficient measured using ^{7}Li exhibits a close proximity to that of the total conductivity. Notably, for the PGE2 electrolyte, these E_a values are found to be equivalent.

The relative hydrodynamic radii of Li$^+$ cations (Table S2) were calculated from the obtained D_s values using the equation $R_{Li} = D_{EMI^+}/D_s$ according to the published method[18] and exhibit a temperature dependence (Figure 3). These calculations were based on the average value of D_s (^{7}Li) [Figure 3(*a*)] and the fast and slow diffusion coefficients measured using ^{7}Li nuclei [Figure 3(*b*)]. As can be seen from Figure 3, an anomalous increase in the R_{Li} value of the Li$^+$ cation is observed in the PGE2 electrolyte with increasing temperature. This phenomenon can be explained by an increase in the population of the slow Li$^+$ cations, which were identified as the main pathway responsible for the transport of the solvated Li$^+$ cation in PGE2.

The NMR relaxation times T_1 and T_2, as well as the line width of the NMR spectrum, are dependent on the modulation frequencies of local interactions, including magnetic dipole–dipole and quadrupole interactions. It is important to note that different relaxation times are sensitive to different frequency ranges of the fluctuation spectrum.[19] The analysis of the temperature dependences of the spin–lattice and spin–spin relaxation times has been recognized to be a reliable method for estimating the correlation times of the local motion of Li$^+$ cations. The elementary jump length *l* was calculated from the Einstein relation using macroscopic diffusion coefficients measured by PFG NMR.†

The calculated temperature dependences of the spin–lattice relaxation times T_1 of the ^{7}Li nuclear spins in both PGE1 and PGE2 compositions demonstrate a decrease with increasing temperature (Figure 4). In the PGE2 composition with G4 the minimum is observed at 50 °C, and in the case of the PGE1 composition with G2 the minimum of the $T_1(T)$ function is not reached in this temperature range.

According to equation (S1),† the minimum is given by $T_1(\omega\tau_{av})^2 \approx 1$ and $\tau_{av} = 10^{-9}$ s. At this temperature, the diffusion coefficient D of the Li$^+$ ion in PGE2 is 7.5×10^{-12} m^2 s^{-1}. The Einstein relation $l = \sqrt{nD\tau_{av}}$ states that the diffusion coefficient D is proportional to the average jump distance *l* of an elementary particle, with the constant *n* equal to 2, 4 or 6 depending on the size of the sample being studied.[20] In our case, $n = 6$. And then for the PGE2 sample, *l* is 0.21 nm, which is close to the length of the Li–O bond.

In order to comprehend the disparities in the mechanism of Li$^+$ cation transport in PGEs with G2 and G4, quantum chemical modeling of the polymer electrolyte composition and Li$^+$ cation transport along the polymer matrix with and without a solvate shell was conducted.

Figure S3(*a*) shows a polymer matrix consisting of four PEGDA chains cross-linked at four different sites by dimerization of the

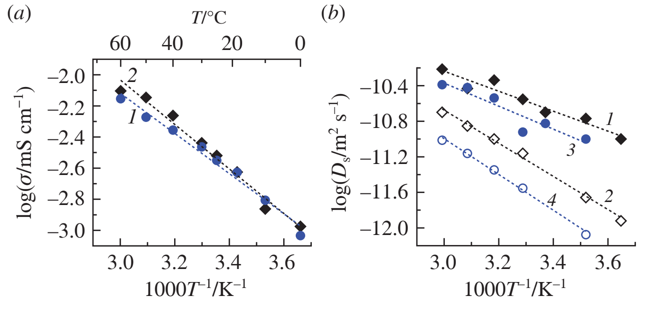

Figure 2 Temperature dependences of the logarithms of (*a*) the conductivity of (*1*) PGE1 and (*2*) PGE2, as well as of (*b*) the (*1*),(*3*) fast and (*2*),(*4*) slow diffusion coefficients D_s in (*1*),(*2*) PGE1 and (*3*),(*4*) PGE2, measured using ^{7}Li nuclei in the temperature range from 0 to 60 °C.

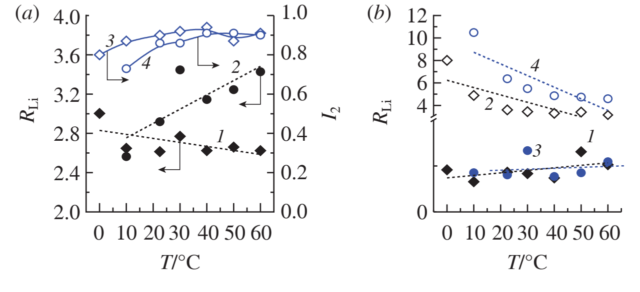

Figure 3 (*a*) Temperature dependences of (*1*),(*2*) relative hydrodynamic radii (R_{Li}) and (*3*),(*4*) populations (I_2) of slow Li$^+$ cations in (*1*),(*3*) PGE1 and (*2*),(*4*) PGE2, measured using ^{7}Li nuclei in the temperature range from 0 to 60 °C. (*b*) Temperature dependence of R_{Li} values of (*1*),(*3*) fast and (*2*),(*4*) slow Li$^+$ cations in (*1*),(*2*) PGE1 and (*3*),(*4*) PGE2.

Table 1 Effective activation energies E_a of conductivity and diffusion coefficients D_s measured using ^{7}Li nuclei.

Electrolyte	Conductivity		D_s (^{7}Li)-fast		D_s (^{7}Li)-slow	
	E_a/kJ mol^{-1}	E_a/eV	E_a/kJ mol^{-1}	E_a/eV	E_a/kJ mol^{-1}	E_a/eV
PGE1	27.4 ± 1.5	0.28 ± 0.01	21.5 ± 2.5	0.22 ± 0.03	35.6 ± 1.4	0.37 ± 0.01
PGE2	24.7 ± 1.3	0.26 ± 0.01	24.7 ± 4.6	0.26 ± 0.05	38.4 ± 1.3	0.40 ± 0.01

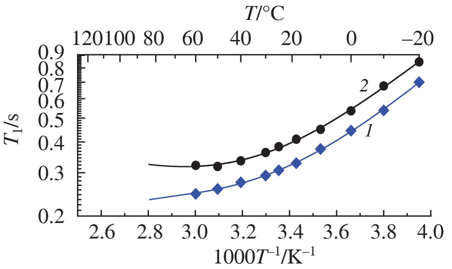

Figure 4 Temperature dependences of the spin–lattice relaxation time T_1 of ^{7}Li nuclei in (*1*) PGE1 and (*2*) PGE2 electrolytes.

acrylate groups. When this matrix is filled with IL molecules [Figure S3(*b*)] and Li^+(G4) solvate complexes, a model of PGE is obtained. The G4 molecule is marked in the figure as it approaches the polymer chain. It is important to note that this figure is illustrative and that quantum chemical calculations, along with determination of the interaction energies of the components, were carried out on simpler models (Figures S4–S6).

Of particular interest is the significant (several times) decrease in the diffusion coefficient of G4 in PGE compared to G2 [Figure 1(*d*)]. Quantum chemical modeling demonstrated that the solvate complexes of the Li^+ cation with G4 [Figure S4(*a*)] interact with the PEO units of the polymer matrix, exhibiting a substantial energy gain of 19 kcal mol^{-1}. Consequently, the formation of mixed complexes is observed [Figures S5(*a*)–(*c*)]. In the case of the solvate complex of Li^+ with two G2 molecules [Figure S4(*b*)], such interaction is accompanied by only a slight decrease in energy and the detachment of one G2 ligand [Figures S5(*d*),(*e*)]. Therefore, the equilibrium constant for the formation of the mixed complex will be significantly higher in the case of G4. As a result, the diffusion of G4 slows down due to the lower mobility of the mixed complex. In the case of fast lithium, the Li^+ ion is transported along the polymer chain (Figure S6).†

The final stage of the work was to investigate the influence of G2 and G4 on the electrochemical properties of PGE. The upper limit of the electrochemical stability window of PGE1 was 3.8 V and that of PGE2 was 4.6 V *vs.* Li/Li^+ [Figure 5(*a*)]. A small peak at 3.5 V *vs.* Li/Li^+, associated with the decomposition of the $EMIBF_4$ IL we neglect, is more pronounced for PGE with G2 than with G4, indicating a stronger binding of the IL in the polymer matrix of PGE2.

EIS measurements of the GPE/Li interface showed that the total resistance of the boundary on the third day of storage was higher for PGE2 than for PGE1 (Figure S7 and Table S3).†

The tests of PGE in the Li/GPE/$LiFePO_4$ cell showed the best stability characteristics for the composition PGE1 with G1 [Figure 5(*b*)]. The decrease in stability for the cell with PGE2 may be due to the higher resistance at the electrode interface, as evidenced by the larger value of the charge–discharge plateau difference in the case of PGE2 (Figure S8).

Thus, it is shown that the macroscopic mass transfer of Li^+ cations is controlled by their solvate environment formed by both solvents (G2 and G4) and the polymer matrix, which in the presence of G4 forms a denser three-dimensional network, which slows down the transport of all ions. Quantum chemical modeling demonstrated that the solvate complexes of the Li^+ cation with G4 interact with the PEO units of the polymer matrix more strongly than those with G2. The electrochemical stability of PGE increases, while the characteristics of the PGE/Li interface deteriorate, which affects the performance of Li/PGE/$LiFePO_4$ cells.

This work was supported by the Ministry of Science and Higher Education of the Russian Federation [project no. 124013000743-3 (FFSG-2024-0008)]. All quantum chemical calculations were performed using the computing capabilities of the Joint supercomputer center of the NRC ‘Kurchatov Institute’.

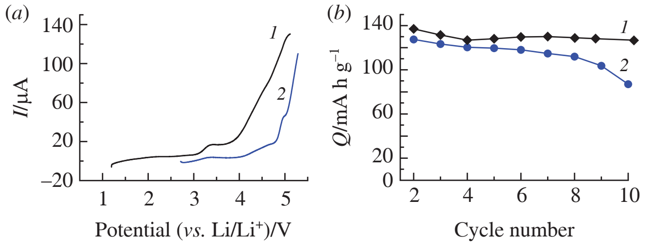

Figure 5 (*a*) Voltammograms of (*1*) Li/PGE1/SS and (*2*) Li/PGE2/SS cells. (*b*) Dependences of discharge capacity on the cycle number for Li//$LiFePO_4$ cells with (*1*) PGE1 and (*2*) PGE2 at a current density of C/10 in the range of 2.6–3.8 V. The specific discharge capacity of the cathode was calculated based on the mass of $LiFePO_4$.

Online Supplementary Materials

Supplementary data associated with this article can be found in the online version at doi: 10.71267/mencom.7792.

References

1 V. I. Volkov, O. V. Yarmolenko, A. V. Chernyak, N. A. Slesarenko, I. A. Avilova, G. R. Baymuratova and A. V. Yudina, *Membranes*, 2022, **12**, 416; https://doi.org/10.3390/membranes12040416.

2 E. Quartarone, S. Davino, E. Lufrano, L. Coppola, C. Simari and I. Nicotera, *ChemElectroChem*, 2023, **10**, e202201148; https://doi.org/10.1002/celc.202201148.

3 P. M. Richardson, A. M. Voice and I. M. Ward, *Polymer*, 2016, **97**, 69; https://doi.org/10.1016/j.polymer.2016.03.074.

4 V. I. Volkov and A. A. Marinin, *Russ. Chem. Rev.*, 2013, **82**, 248; https://doi.org/10.1070/RC2013v082n03ABEH004278.

5 N. A. Slesarenko, A. V. Chernyak, K. G. Khatmullina, G. R. Baymuratova, A. V. Yudina, G. Z. Tulibaeva, A. F. Shestakov, V. I. Volkov and O. V. Yarmolenko, *Membranes*, 2023, **13**, 776; https://doi.org/10.3390/membranes13090776.

6 K. G. Khatmullina, N. A. Slesarenko, A. V. Chernyak, G. R. Baymuratova, A. V. Yudina, M. P. Berezin, G. Z. Tulibaeva, A. A. Slesarenko, A. F. Shestakov and O. V. Yarmolenko, *Membranes*, 2023, **13**, 548; https://doi.org/10.3390/membranes13060548.

7 O. V. Yarmolenko, K. G. Khatmullina, G. R. Baymuratova, N. A. Emelianov, R. K. Baimuratova and A. V. Yudina, *High Energy Chem.*, 2023, **57**, S375; https://doi.org/10.1134/S0018143923080258.

8 Y. Pei, Y. Zhang, J. Ma, M. Fan, S. Zhang and J. Wang, *Mater. Today Nano*, 2022, **17**, 100159; https://doi.org/10.1016/j.mtnano.2021.100159.

9 H. Gupta and R. K. Singh, in *Energy Storage Battery Systems: Fundamentals and Applications*, eds. S. Haider, A. Haider, M. Khodaei and L. Chen, IntechOpen, London, 2021, ch. 5; https://doi.org/10.5772/intechopen.93397.

10 H. Qi, Y. Ren, S. Guo, Y. Wang, S. Li, Y. Hu and F. Yan, *ACS Appl. Mater. Interfaces*, 2020, **12**, 591; https://doi.org/10.1021/acsami.9b16786.

11 A. K. Tripathi, *Mater. Today Energy*, 2021, **20**, 100643; https://doi.org/10.1016/j.mtener.2021.100643.

12 K. Karuppasamy, J. Theerthagiri, D. Vikraman, C.-J. Yim, S. Hussain, R. Sharma, T. Maiyalagan, J. Qin and H.-S. Kim, *Polymers*, 2020, **12**, 918; https://doi.org/10.3390/polym12040918.

13 X. Wang, L. Jin, W. Feng, Z. Zhou and H. Zhang, *Sci. China: Chem.*, 2023, **66**, 3443; https://doi.org/10.1007/s11426-023-1827-0.

14 K. Shigenobu, T. Sudoh, J. Murai, K. Dokko, M. Watanabe and K. Ueno, *Chem. Rec.*, 2023, **23**, e202200301; https://doi.org/10.1002/tcr.202200301.

15 W. A. Henderson, *J. Phys. Chem. B*, 2006, **110**, 13177; https://doi.org/10.1021/jp061516t.

16 K.-J. Suh, Y.-S. Hong, V. D. Skirda, V. I. Volkov, C.-Y. J. Lee and C.-H. Lee, *Biophys. Chem.*, 2003, **104**, 121; https://doi.org/10.1016/S0301-4622(02)00361-7.

17 K. Hayamizu and Y. Aihara, *Electrochim. Acta*, 2004, **49**, 3397; https://doi.org/10.1016/j.electacta.2004.03.007.

18 K. Hayamizu and E. Akiba, *Electrochemistry*, 2003, **71**, 1052; https://doi.org/10.5796/electrochemistry.71.1052.

19 A. Kessenikh, *Substantia*, 2021, **5** (2), 19; https://doi.org/10.36253/Substantia-1224.

20 J. T. Edward, *J. Chem. Educ.*, 1970, **47**, 261; https://doi.org/10.1021/ed047p261.

Received: 4th April 2025; Com. 25/7792